한국표면공학회지
J. Kor. Inst. Surf. Eng.
Vol. 47, No. 5, 2014.
http://dx.doi.org/10.5695/JKISE.2014.47.5.252

<연구논문>

High-temperature Oxidation of the TiAlCrSiN Film Deposited on the Cemented Hard Carbide

Dong Bok Lee*

School of Advanced Materials Science & Engineering, Sungkyunkwan University, Suwon 440-746, Korea

(Received October 8, 2014 ; accepted October 23, 2014)

Abstract

The TiAlCrSiN film was deposited on the WC-20%TiC-10%Co carbide, and its oxidation behavior was examined at 700-1000°C. It displayed relatively good oxidation resistance owing to the formation of TiO_2, Al_2O_3, Cr_2O_3, and SiO_2 up to 900°C. However, at 1000°C, the fast oxidation rate and partial oxidation of WC in the substrate led to the formation of the thick, fragile oxide scale.

Keywords: TiAlCrSiN film; WC-TiC-Co cemented hard carbide; Cathodic arc plasma deposition; Oxidation

1. Introduction

TiCrAlSiN films were developed in order to improve the high-temperature oxidation resistance, corrosion resistance, and mechanical properties of conventional TiN films that are widely used as hard films to protect and increase the lifetime and performance of cutting tools or die molds.[1)] As listed in Table 1[2-10)], TiCrAlSiN films were deposited on WC-Co cemented carbides, Si, Pt, and steel substrates, and their microstructures[2-5,7,8)], mechanical properties including microhardness[2,3,5,8)] wear[10)] and cutting performance[7)], and thermal stability in vacuum[2,3)] or air[4,6,7)] were studied. The air-oxidation behavior was studied for 0.5 - 2 h between 800 and 1000°C[4,6,7,9)]. The oxidation characteristics of the films depend sensitively on the deposition method and parameters that affect their crystallinity, composition, stoichiometry, thickness, surface roughness, grain size and orientation. Hence, it is necessary to study the high-temperature oxidation behavior of the TiAlCrSiN films under diverse oxidizing conditions. On the hand, cemented carbides consist of hard and wear resistant WC refractory particles and the tough, ductile Co binder phase. They have been used as cutting tools, rock drill tips, and structural components in machinery for decades[11)]. The addition of the cubic TiC carbide in WC–Co enhances the hardness and wear resistance of cemented carbides. TiAlCrSiN films that deposited on cemented carbides could be used in abrasive and corrosive environments. However, they are inevitably degraded by the high-temperature oxidation during service. Hence, the TiAlCrSiN nano-multilayered film was deposited on WC-TiC-Co cemented carbide, and its high-temperature oxidation behavior was examined. The oxidation resistance is a key factor in determining the service lifetime.

2. Experimental

The TiAlCrSiN film was deposited on WC-20% TiC-10%Co cemented carbide substrate using 70 at.%Ti-30 at.%Cr and 88 at.%Al-12 at.%Si alloys as cathodes by cathodic arc plasma deposition[8,9)]. Its composition was 13.5Ti-9.3Al-5.9Cr-1.5Si-69.8N (at%). The nano-multilayered structure was obtained by rotating the substrate between two opposing Ti-Cr and Al-Si alloy cathodes at 4.55 rpm, while maintaining the nitrogen pressure at 4 Pa, temperature at 300°C, bias voltage at −100 V, Ti-Cr arc current at 55 A, and Al-Si arc current at 50 A. The TiAlCrSiN film oxidized at 700 - 1000°C for 10 h in air, and inspected by a scanning

*Corresponding author. E-mail : dlee@skku.ac.kr

Table 1. Deposition condition and phases present in the TiCrAlSiN films

films/ deposition method	substrate	target	phase present
(Ti,Cr,Al,Si)N/ cathodic arc deposition[2)]	WC-Co	TiCrAlSi	*hcp*- & *fcc*-TiCrAlSiN
(Ti,Cr,Al)N/(Al,Si)N nano-multilayers/ arc ion plating[3)]	Si, WC-Co	TiCrAl, AlSi	*hcp*-(Al,Si)N & *fcc* -(Ti,Cr,Al)N
TiAlSiN/CrAlN nano-multilayers/ arc ion plating[4)]	Si, WC-Co	TiAlSi, CrAl	*fcc*-TiAlSiN & *fcc*-CrAlN
(Ti,Cr,Al,Si)N with a columnar structure/ cathodic arc deposition[5)]	WC-Co, Si	TiCrAlSi	*hcp*- & *fcc*-TiCrAlSiN
CrTiAlSiN with a columnar structure/ cathodic arc deposition[6)]	Si	Cr, Ti, AlSi	*fcc*-(Cr,Ti)N
(Ti,Cr,Al,Si)N nanocrystalline/ arc ion plating[7)]	WC-Co, Pt	TiCrAlSi	*hcp*- & *fcc*-TiCrAlSiN
TiAlCrSiN nano-multilayers/ cathodic arc deposition[8,9)]	tool steel	TiCr, AlSi	Ti(Cr)N & Al(Si)N
TiAlCrSiN nano-multilayers/ magnetron sputtering[10)]	tool steel	Ti, Cr, Al, Si	(Al, Ti, Si)N & CrN

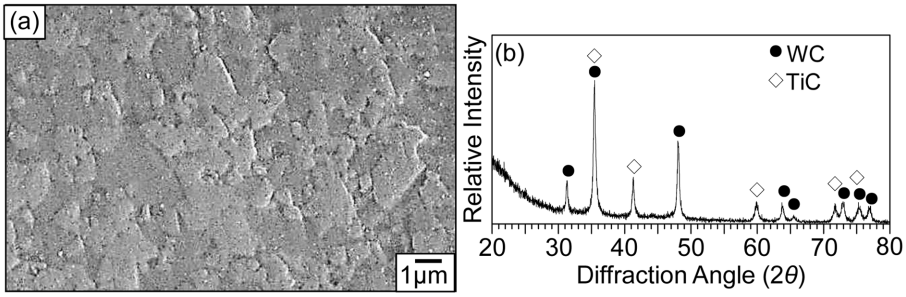

Fig. 1. WC-20%TiC-10%Co substrate. (a) SEM microstructure, (b) XRD pattern.

electron microscope (SEM), a transmission electron microscope (TEM), an X-ray diffractometer (XRD), and an electron probe microanalyzer (EPMA).

3. Results and Discussion

Fig. 1 shows SEM/XRD results of the WC-20TiC-10Co substrate. WC and TiC particles were embedded in the Co binder (Fig. 1(a)). In Fig. 1(b), α–WC and the TiC additive were detected, but Co was not detected due to its small amount.

Fig. 2 shows SEM/TEM/XRD results of the Ti AlCrSiN film deposited on the substrate. Some microdroplets scattered over the film surface with a ridge microstructure (Fig. 2(a)). The compact film was about 6 μm thick (Fig. 2(b)). It had a nano-multilayered structure (Fig. 2(c)). The white nanolayers were TiN containing some Cr, and the dark nanolayers were AlN containing some Si (Fig. 2(d)). Such a contrast effect occurred because Al has a lower scattering factor than Ti. In Fig. 2(e), α–WC, TiC, and TiN were detected, but their diffraction patterns were weak and broad, because the film had a nanostructure. AlN was not detected in Fig. 2(e), because its amount was smaller than that of TiN.

Fig. 3 shows SEM/EPMA results of the TiAlCrSiN film deposited on the substrate after oxidation at 700°C for 10 h. The surface morphology of the film shown in Fig. 3(a) was similar to that shown in Fig. 2(a), owing to the small extent of oxidation. About 1 μm-thick oxide sale formed on the retained film (Fig. 3(b)). The oxide scale, the TiAlCrSiN film, and the WC-20TiC-10Co substrate were recognizable in Fig. 3(c). During oxidation, nitrogen escaped into the air from the surface. Similar results were obtained when the TiAlCrSiN film oxidized at 800°C for 10 h.

Fig. 4 shows SEM/EDS results of the TiAlCrSiN film deposited on the substrate after oxidation at 900°C for 10 h. In Fig. 4(a), the surface ridge structure was no longer visible, and the scale spalled locally. Numerous tiny oxide grains shown in Fig. 4(a) indicate that the TiAlCrSiN film had a good oxidation resistance due to the presence of Ti, Al, Cr, and Si. These elements would form the highly stoichiometric, protective oxides of Al_2O_3, Cr_2O_3, and SiO_2, besides the semiprotective, nonstoichiometric TiO_2. These oxide phases were however not able to be identified using XRD, owing to the partial breakage of the thin scale and the film. Such mechanical failure shown in Fig. 4(b) resulted from the hardness mismatch among the oxides with a limited plasticity, the superhard film (max. hardness of 43 GPa),[8)] and the hard cemented carbide substrate. To get the image of Fig. 4(b), it

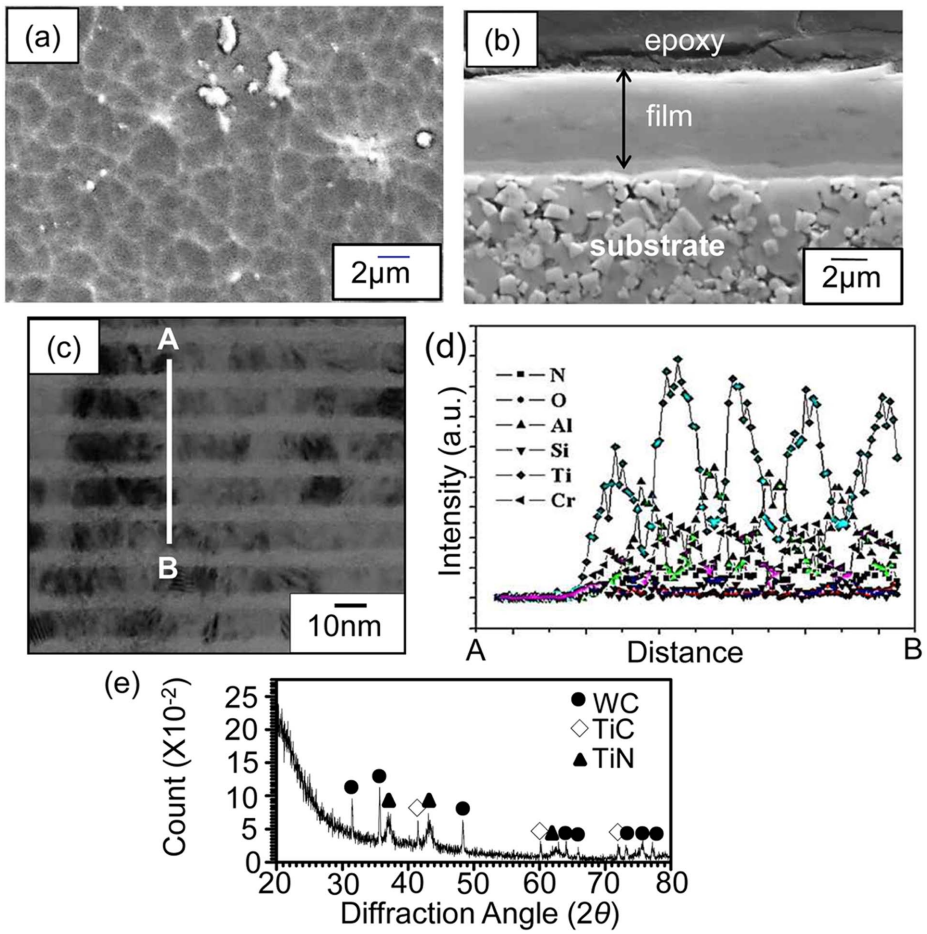

Fig. 2. TiAlCrSiN film deposited on the WC-20%TiC-10%Co substrate. (a) SEM top view, (b) SEM cross-sectional image, (c) TEM cross-sectional image. (d) EDS line profiles along A-B. (e) XRD pattern.

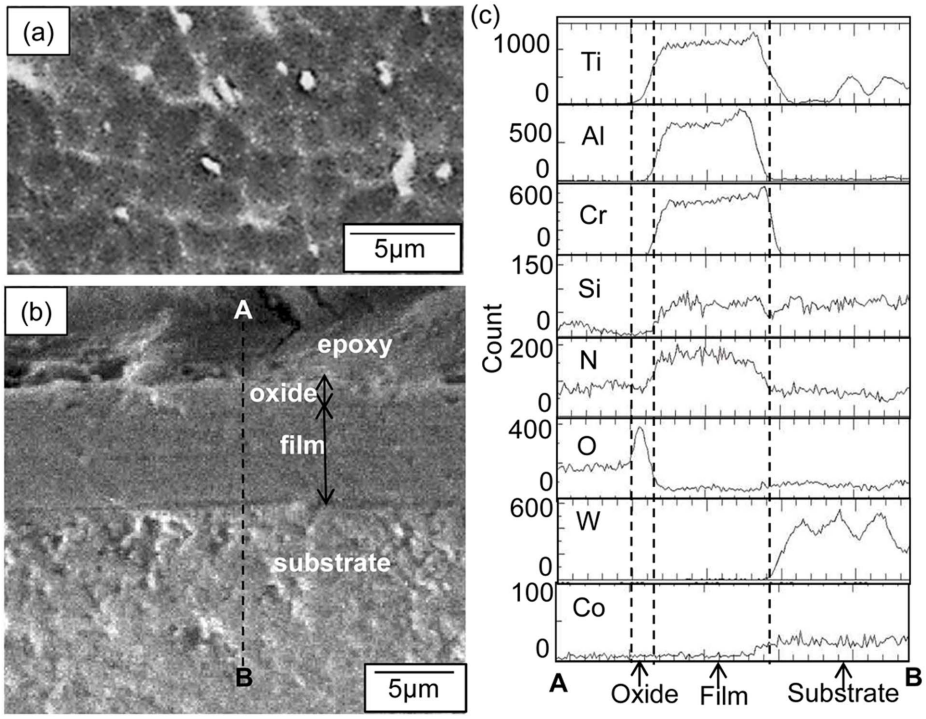

Fig. 3.TiAlCrSiN film after oxidation at 700°C for 10 h. (a) SEM top view, (b) EPMA cross-sectional image, (c) EPMA line profiles along A-B.

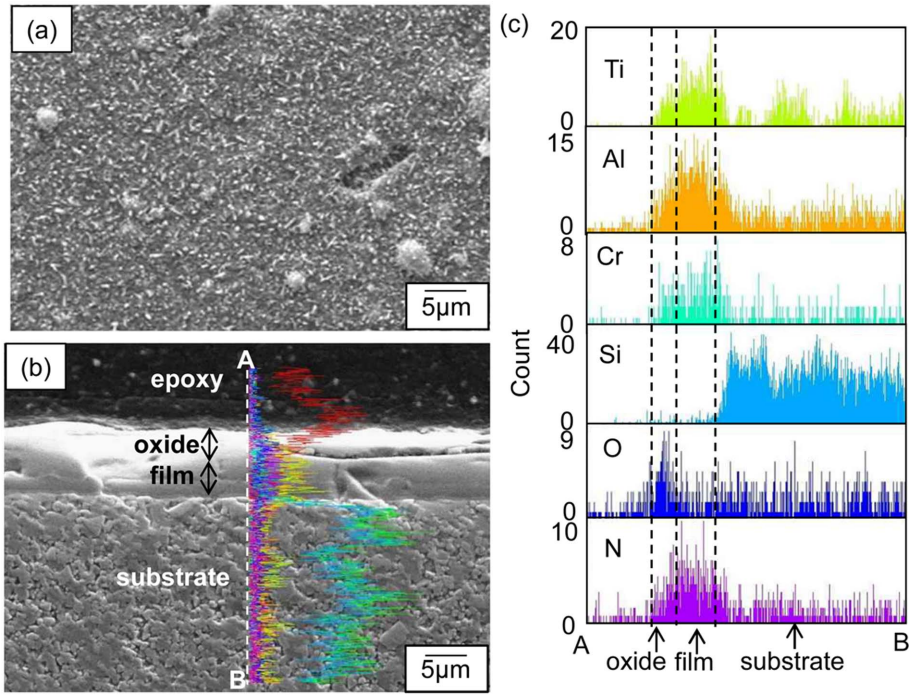

Fig. 4. TiAlCrSiN film after oxidation at 900°C for 10 h. (a) SEM top view, (b) SEM cross-sectional image, (c) EDS line profiles along A-B.

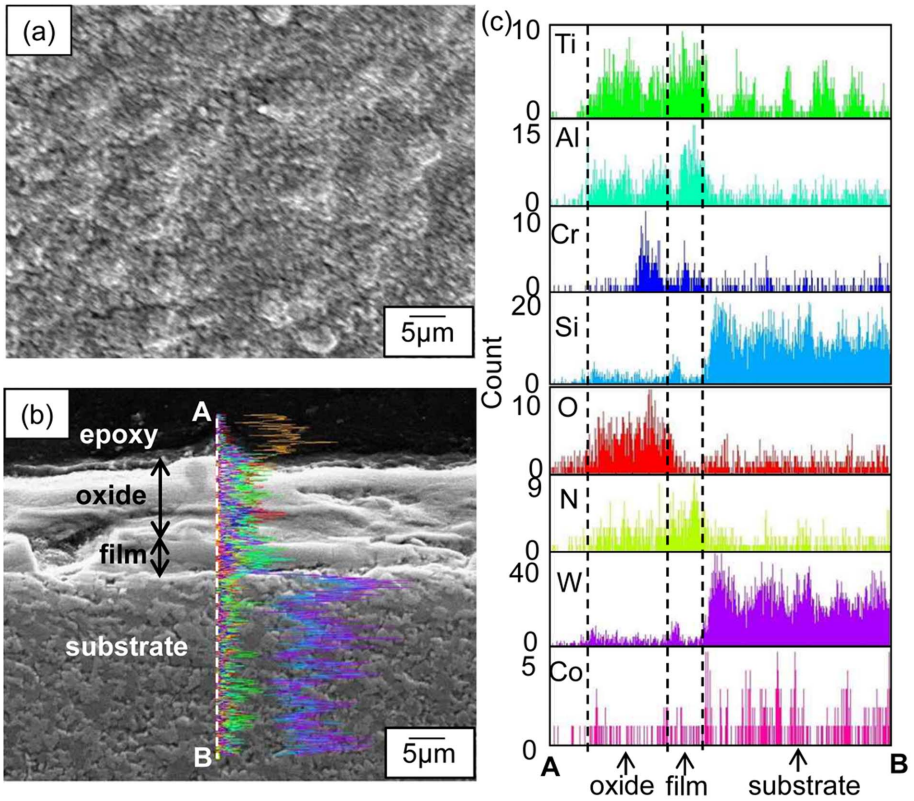

Fig. 5. TiAlCrSiN film after oxidation at 1000°C for 10 h. (a) SEM top view, (b) SEM cross-sectional image, (c) EDS line profiles along A-B.

took rather long time to polish the wear-resitant substrate. The oxide scale was about 2 μm thick (Fig. 4(b)). Despite the high oxidizing temperature of 900°C, nitrogen still remained in the unoxidized TiAlCrSiN film (Fig. 4(c)).

Fig. 5 shows SEM/EDS results of the TiAlCrSiN

film deposited on the substrate after oxidation at 1000°C for 10 h. Fig. 5(a) shows the oxide surface morphology. The surface was not flat, and the surface oxide consisted of numerous tiny oxide grains, which were bigger than the surface oxide grains shown in Fig. 4(a). The oxide scale that formed on the film was about 10 μm thick (Fig. 5(b)). The oxidation of the film led to the volume expansion to make the thick oxide scale. Both the oxide scale and the film were partially broken due to the mechanical weakness. In Fig. 5(c), Cr_2O_3 formed at the lower part of the (TiO_2, Al_2O_3)-mixed scale. This suggested that the oxygen active elements of Ti and Al oxidized preferentially at the surface, which resulted in the enrichment and thereby the oxidation of Cr underneath. Some W was incorporated in the film and the oxide scale (Fig. 5(c)). It is known that WC(s) oxidizes to volatile tungsten-oxides such as WO, WO_2, and WO_3, being accompanied with a large volume expansion and evolution of CO and CO_2 gases.[12] Hence, W can be incorporated in the oxide scale. These facts aggravated the mechanical integrity of the oxide layer and the film. Hence, the thick, fragile oxide scale formed at 1000°C.

4. Summary

The nanomultilayered TiAlCrSiN film was deposited on WC-20%TiC-10%Co cemented carbide substrate by cathodic arc plasma deposition. It displayed relatively good oxidation resistance at 700-900°C, owing to the formation of protective oxides of Al_2O_3, Cr_2O_3, and SiO_2, together with semiprotective TiO_2. At 1000°C, the increased temperature and WC in the substrate led to the formation of the imperfect oxide scale that consisted primarily of the outer (TiO_2, Al_2O_3)-mixed scale and inner (TiO_2, Al_2O_3, Cr_2O_3)-mixed scale.

Acknowledgments

This work was supported by the Human Resource Development Program (No. 20134030200360) of the Korea Institute of Energy Technology Evaluation and Planning (KETEP) grant funded by the Korea government Ministry of Trade, Industry and Energy.

References

1. A. D. Pogrebnjak, A. V. Pshyk, V. M. Beresnev, B. R. Zhollybekov, J. Frict. Wear, 35, (2014) 55.
2. H. Ezura, K. Ichijo, H. Hasegawa, K. Yamamoto, A. Hotta, T. Suzuki, Vacuum 82 (2008) 476.
3. N. Fukumoto, H. Ezura, K. Yamamoto, A. Hotta, T. Suzuki, Surf. Coat. Technol. 203 (2009) 1343.
4. N. Fukumoto, H. Ezura, T. Suzuki, Surf. Coat. Technol. 204 (2009) 902.
5. K. Ichijo, H. Hasegawa, T. Suzuki, Surf. Coat. Technol. 201 (2007) 5477.
6. Y. Y. Chang, C. Y. Hsiao, Surf. Coat. Technol. 204 (2009) 992.
7. K. Yamamoto, S. Kujime, K. Takahara, Surf. Coat. Technol. 200 (2005) 1383.
8. S. K. Kim, P. V. Vinh, J. W. Lee, Surf. Coat. Technol. 202 (2008) 5395.
9. T. D. Nguyen, S. K. Kim, D. B. Lee, Surf. Coat. Technol. 204 (2009) 697.
10. R. P. Martinho, M. F. C. Andrade, F. J. G. Silva, R. J. D. Alexandre, A. P. M. Baptista, Wear, 267 (2009) 1160.
11. S. N. Basu, V. K. Sarin, Mater. Sci. Eng. A, 209 (1996) 206.
12. Y. S. Hwang, D. B. Lee, Adv. Mater. Res. 811 (2013) 93.